Tailor-Made Iridium Oxide (IrOx) Coated Titanium Electrode: pH Sensor towards Potentiometric Titration

Hoa-Hung Lam[a,b], Hong-Phuong Phan[a,b], Trung Dang-Bao[a,b,*]

[a]Faculty of Chemical Engineering, Ho Chi Minh City University of Technology (HCMUT), 268 Ly Thuong Kiet Street, District 10, Ho Chi Minh City, Vietnam
[b]Vietnam National University Ho Chi Minh City, Linh Trung Ward, Thu Duc City, Ho Chi Minh City, Vietnam
 dbtrung@hcmut.edu.vn

In this work, the pH sensor electrode based on iridium oxides (IrO_x) was developed and applied to potentiometric titration, instead of the traditional glass membrane electrodes, with its dominant features such as easy-implementation, low-cost and small-size. The electrode consisting of the IrO_x layered on the surface of titanium substrate was fabricated by an anodizing method. Such electrode (IrO_x/Ti) was highly sensitive to a pH change in a solution, but not in the presence of oxidizing or reducing agents. With the aim to minimize these chemical interferences, the IrO_x/Ti electrode was covered by a nafion thin-film via a dip-coating method, namely Nf-IrO_x/Ti. Besides the high mechanical stability, the Nf-IrO_x/Ti sensing electrode indicated a linear correlation between the potential and the solution pH in the range of pH 2−12, with the response time of 120 s for an equilibrium. Although the response time of such pH electrode was quite longer than those of IrO_x/Ti (60 s) and the commercial glass membrane electrode (30 s), the Nf-IrO_x/Ti electrode permitted determining the equivalence points in acid-base potentiometric titrations with a high accuracy (less than 1 % relative errors in comparison with the corresponding values obtained by the commercial glass membrane electrode).

1. Introduction

The pH determination plays an important analytical technique in agriculture (Fan et al., 2018), wastewater treatment, pharmaceuticals and foodstuffs (Salvo et al., 2017). In the field of medicine, pH value is also an important parameter in blood specimens based on pH-dependent biochemical reactions in living organisms. As a conventional tool, the pH glass membrane electrodes have been most frequently used thanks to their simplicity. Such glass-type electrodes are incompatible to hydrofluoric acid and alkaline solutions, occurring large errors (Xi et al., 2021). In particular, glass electrodes present their irreparable limits in pH determination in micro-scale systems or in vivo studies, caused by their vulnerability and impossibility in miniaturization (Mani et al., 2017).

The pH microsensors based on transition metal oxides have paid a great attention thanks to their highly proton-sensitive property (Manjakkal et al., 2020). Among other, iridium oxides were evidenced as efficient pH sensors, mainly attributed to the chemical transformation between Ir(IV) and Ir(III) species depending on pH conditions (Zhou et al., 2020). Such pH sensors adapt the technical requirements such as rapid response time, Nernstian pH response, non-toxicity and handling in micro-sizes, widening their applications in certain systems, particularly in living organisms. In general, iridium oxides layer could be fabricated by thermal oxidation (Ratanaporncharoen et al., 2018), sputtering deposition (Xi et al., 2021) or electrochemical method (Jang and Lee, 2020). Some drawbacks can be raised from such above-mentioned methods; for example, thermal oxidation requires high working-temperatures (400−900 °C), sputter deposition requires highly controlled fabrication parameters and gives a high cost. The recent achievements of nanotechnology have widened the possibilities in fabrication and applications of metal and metal oxide nanoparticles (Dang-Bao et al., 2022).

The aim of this paper was to present easy-implementation and low-cost approach to fabricate IrO_x coated titanium electrode via an anodizing method. The comparative study in potential response between nafion-coated IrO_x electrode and non-coated IrO_x electrode was also examined, permitting expanding the application of such

electrodes in real aqueous samples. The as-prepared electrodes were applied to various acid-base potentiometric titrations in order to evaluate the potential-pH linear correlation, the response time and the accuracy compared to the glass-type pH electrode.

2. Experimental

2.1 Fabrication of IrO$_x$/Ti and Nf-IrO$_x$/Ti electrodes

Preparation of electrolyte solution (Kim and Yang, 2014) with some modifications: IrCl$_4$.xH$_2$O (75 mg) was dissolved in 50.0 mL of distilled water. Adding 0.50 mL hydrogen peroxide (30 %, w/w) and 365 mg oxalic acid dihydrate into the solution and stirring for 30 min. Afterwards, the pH solution was adjusted at pH 10.5 using anhydrous potassium carbonate to obtain the yellow solution. The solution was aged at 90 °C for 10 min and the color was changed to dark blue. Finally, the solution was stored at 4 °C for 1 mth using.

Fabrication of IrO$_x$/Ti electrode: titanium wire (1.0 mm in diameter) was cleaned by removing titanium oxide on its surface using sandpaper and soaking in a solution of 50.0 g/L NaOH and 5.0 g/L washing powder, ultrasonicated for 10 min and then rinsed with distilled water. The surface of such titanium wire was continuously activated by soaking in an acid solution (100.0 g oxalic acid and 5.0 mL concentrated HCl dissolved in 1.0 L distilled water) at 60−80 °C for 20 min and then rinsed with distilled water. The iridium oxides layer was deposited on titanium wire using a constant potential deposition in a 75 mL glass cell containing 50 mL of the electrolyte solution. A U-shaped platinum coated tantalum (10 mm × 30 mm) was used as a cathode. A constant potential of 0.6 V versus Ag/AgCl (3.0 M KCl) for 10 min was optimal for the formation of dark greenish-blue IrO$_x$ on titanium substrate. After rinsing with distilled water, titanium remained parts were covered by epoxy resin and then dried at 80 °C for 1 h. The final electrode was twice soaked in distilled water for 1 d before using.

Fabrication of Nf-IrO$_x$/Ti electrode: the as-prepared IrO$_x$/Ti electrode was soaked in 2 wt% nafion solution (dissolved in isopropanol) for 10 s, and then dried at 50 °C. The nafion coating step was replicated twice before harmonizing in 3.0 M KCl solution for 2 d.

2.2 Potential responses of IrO$_x$/Ti and Nf-IrO$_x$/Ti electrodes towards pH

The IrO$_x$/Ti (or Nf-IrO$_x$/Ti) as an indicator electrode and Ag/AgCl as a standard electrode were placed in the pH buffer solution and connected to a potentiometer. The potentials were recorded in each 5 s until reaching the unchanged potential in next 20 s. Plot the measured potentials (E, mV) against the measured pH value, and explore the linearity of the E = f(pH) curve.

2.3 Acid-base potentiometric titration using Nf-IrO$_x$/Ti electrode

Titration system consisted of burette containing titrant (a standard solution of 0.100 N HCl or 0.100 N NaOH), beaker containing an accurate volume of an unknown-concentration sample, Nf-IrO$_x$/Ti as an indicator electrode and Sentek salt bridge Ag/AgCl as a reference electrode. The two electrodes were placed in an unknown-concentration solution (contained in a beaker and stirred) and connected to a potentiometer. Once stabilizing, the potential was labelled the initial value (E$_0$, mV) in the absence of the titrant volume (V$_{titrant}$ = 0.00 mL). The titration was carried out by gradually adding a titrant to a measured solution, the corresponding potentials were recorded until reaching the equivalence point and kept recording the next 4−5 values (taking reading the potentials every 0.10 mL of a standard solution). The titration curves were plotted between E (mV) versus titrant volume (mL) added and the equivalence points were determined by an interpolation method (Harvey, 2000). In fact, the maximum at the first derivative plot (ΔE/ΔV versus V) or the intersection point between the second derivative plot (Δ^2E/ΔV^2 versus V) and the horizontal axis permitted determining the equivalence point. In this study, the second derivative plot was used as the following Eq(1).

$$V_{eq} = V_{bf} + 0.10 \times \frac{\dfrac{\Delta^2 E}{\Delta V^2}(bf)}{\dfrac{\Delta^2 E}{\Delta V^2}(bf) + \dfrac{\Delta^2 E}{\Delta V^2}(af)} \qquad (1)$$

Where V$_{eq}$ and V$_{bf}$ represent volumes of titrant at the equivalence point and before the equivalence point; Δ^2E/ΔV^2 (bf) and Δ^2E/ΔV^2 (af) represent the second derivative plot values before and after the equivalence point.

3. Results and Discussion

3.1 Characteristics and potential responses of IrO$_x$/Ti and Nf-IrO$_x$/Ti electrodes towards pH

The IrO$_x$/Ti electrode was characterized by scanning electron microscope (SEM), evidencing the formation of iridium oxide spheres with average size of 100 nm and their well-dispersion on the surface of titanium wire in

comparison with the uncoated titanium surface (Figure 1a and 1b). X-ray fluorescence (XRF) elemental analysis also confirmed the presence of iridium on the electrode surface along with electro-conductive titanium base (Figure 1c). To sum up, the iridium oxide layer was successfully fabricated on the titanium wire using an anodizing method.
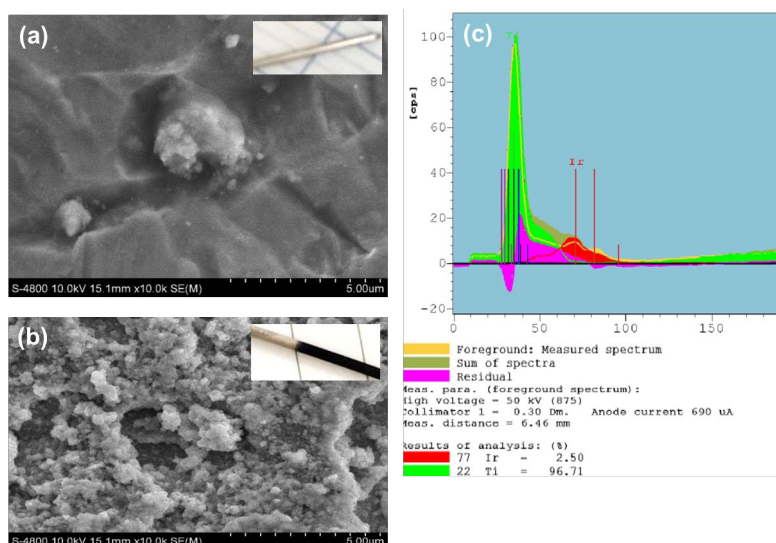

Figure 1: SEM micrographs (scale bar = 5.00 μm) of (a) uncoated titanium wire and (b) fabricated IrO$_x$/Ti electrode with the corresponding images inserted; (c) XRF elemental analysis of fabricated IrO$_x$/Ti electrode

The potential response of IrO$_x$/Ti electrode towards pH was performed in triplicate, evidencing the linear correlation between the potential and the solution pH in the pH range of 2–12 (Figure 2a). In more details, the slopes of the potential curves towards pH were negative and varied from 59 to 61 mV/pH, being slightly greater than an ideal value of approximately 59.12 mV/pH at 25 °C (Manjakkal et al., 2020). This result was close to the Nernstian pH response; meanwhile, the previous reports on various IrO$_2$ sensors showed their sensitivities of 51.1 mV/pH at pH 1.5–12 (by a dip coating method) (Huang et al., 2011), and 72.9 mV/pH at pH 3–11 (by an electrodeposition method) (Prats-Alfonso et al., 2013). The pH response mainly refers to ion exchange on the surface of IrO$_x$ consisting of hydroxyl groups (from adsorbed water), leading to the formation of a couple of metal oxides and their difference in potential. At pH < 2 or pH > 12, the use of IrO$_x$/Ti electrode could be restricted due to the fact that titanium substrate can be corrosive in a strong acidic or an alkaline solution.
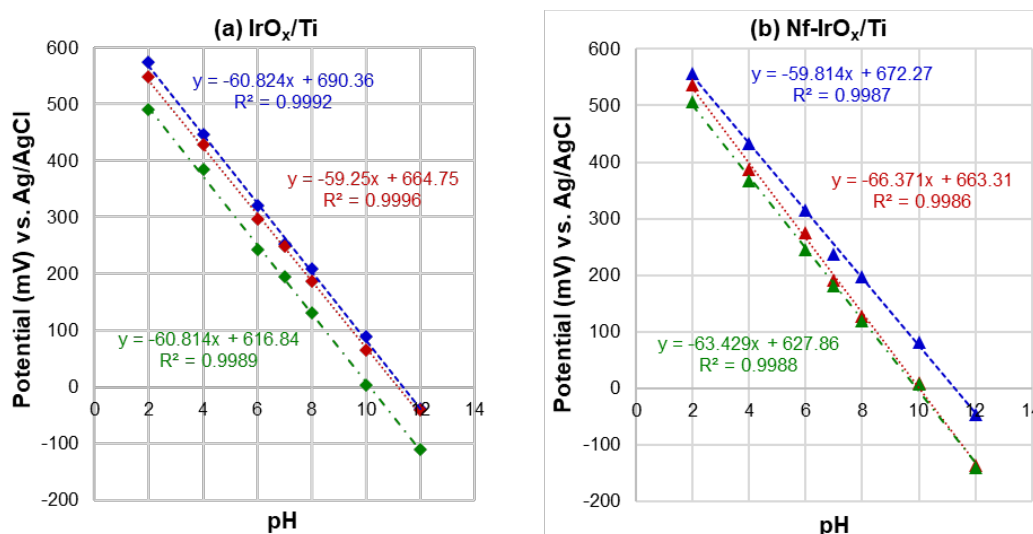

Figure 2: Potential response of (a) IrO$_x$/Ti and (b) Nf-IrO$_x$/Ti electrodes towards pH (different colours represent triplicate experiments)

In order to expand the application of such an electrode in real samples, the IrO_x film should be protected from mechanical impacts or chemical interferences with oxidizing agents (such as dissolved oxygen, H_2O_2, chlorine in water), reducing agents (organic substances, sulphites) or insoluble scales shielding the film. In this study, the IrO_x/Ti electrode was coated with a nafion film; in which, nafion polymer could act as a proton-exchange membrane, but it also prevented the exchange of other substances (Shylendra et al., 2023). The potential responses towards the solution pH of Nf-IrO_x/Ti electrode were triplicated (Figure 2b), evidencing the similar results as those of IrO_x/Ti electrode (linear correlation in the pH range of 2−12, negative slopes varied from 59 to 66 mV/pH).

The potential responses towards time of both IrO_x/Ti and Nf-IrO_x/Ti electrodes were indicated in Figure 3. For IrO_x/Ti electrode, the potential response changed rapidly within the first 30 s, and could reached an equilibrium within the further 30 s; the equilibrium potential could be recorded within 60 s. When anodizing titanium, it was possible that a very small amount of metal oxide could be formed in the innermost layer before the IrO_x layer was formed. The total potential response of the electrode could be the sum of the potential of Ir(IV)/Ir(III) in the IrO_x and the potential of TiO_x/Ti in the substrate (Kim and Yang, 2014).

The major difference between Nf-IrO_x/Ti and IrO_x/Ti electrodes relied on the potential response towards time (Figure 3). In most cases of the pH conditions, the nafion coated electrode took place a longer time for the response potential to reach an equilibrium. In a range of pH < 6, the potential responses of Nf-IrO_x/Ti took place 30−60 s to reach an equilibrium, being similar to IrO_x/Ti electrode. At acidic pH conditions, the proton exchange across the nafion membrane is fast enough, the response time can be slightly slower than that of uncoated nafion electrode. In a range of pH 7−12, the potential response took place 60−120 s to reach an equilibrium. It could be because the proton concentration was too low, leading a slower proton exchange between the solution and the nafion membrane. It should be noted that, in an alkaline environment, proton could move back the solution from the nafion membrane because the proton concentration in the solution was too low, which generated a driving force for the deprotonation of $-SO_3H$ groups, and then the nafion membrane was negatively charged and neutralized by cations (Na^+, K^+, Ca^{2+} or Mg^{2+}) (Zhu et al., 2022). When using Nf- IrO_x/Ti electrode, the equilibrium potential should be recorded after 120 s. In an acid-base potentiometric titration, the equilibrium time can be extended from 1 to 5 min.
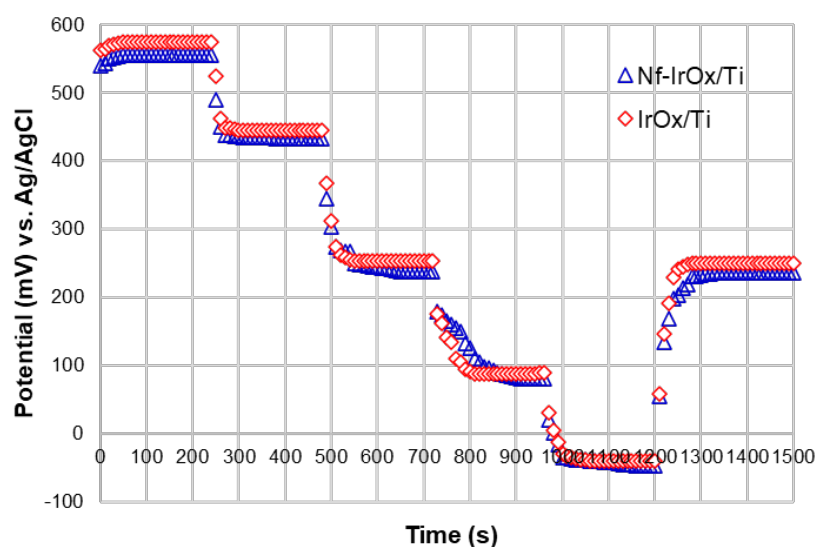

Figure 3: Potential response of (a) IrO_x/Ti and (b) Nf-IrO_x/Ti electrodes towards time at pH 2 (0–4 min), pH 4 (4−8 min), pH 7 (8−12 min), pH 10 (12−16 min), pH 12 (16–20) and return to pH 7 (20–24 min)

3.2 Acid-base potentiometric titration using Nf-IrO_x/Ti electrode

In this section, the Nf-IrO_x/Ti electrode was applied as an indicator electrode in an acid-base potentiometric titration, using either 0.100 N NaOH or 0.100 N HCl solution as a titrant. Acting as an indicator electrode, Nf-IrO_x/Ti electrode indicated higher potentials than glass membrane pH electrode with similar acid-base titration curves, involving the titrations of a strong acid (HCl) and a polyprotic acid (H_3PO_4) by a strong base (NaOH) (Figure 4), and the titrations of polybasic bases (Na_2CO_3 and $Na_4P_2O_7$) by a strong acid (HCl) (Figure 5).
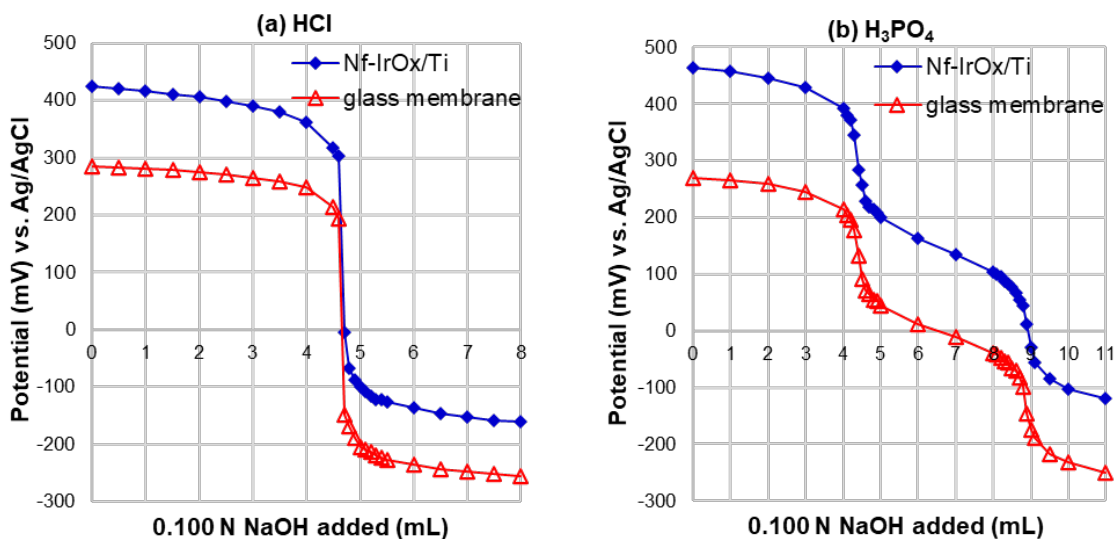
Figure 4: *Potentiometric titration curves between 0.100 N NaOH and (a) HCl and (b) H_3PO_4 using Nf-IrO$_x$/Ti and traditional glass membrane electrodes (Sentix-41 combination electrode)*
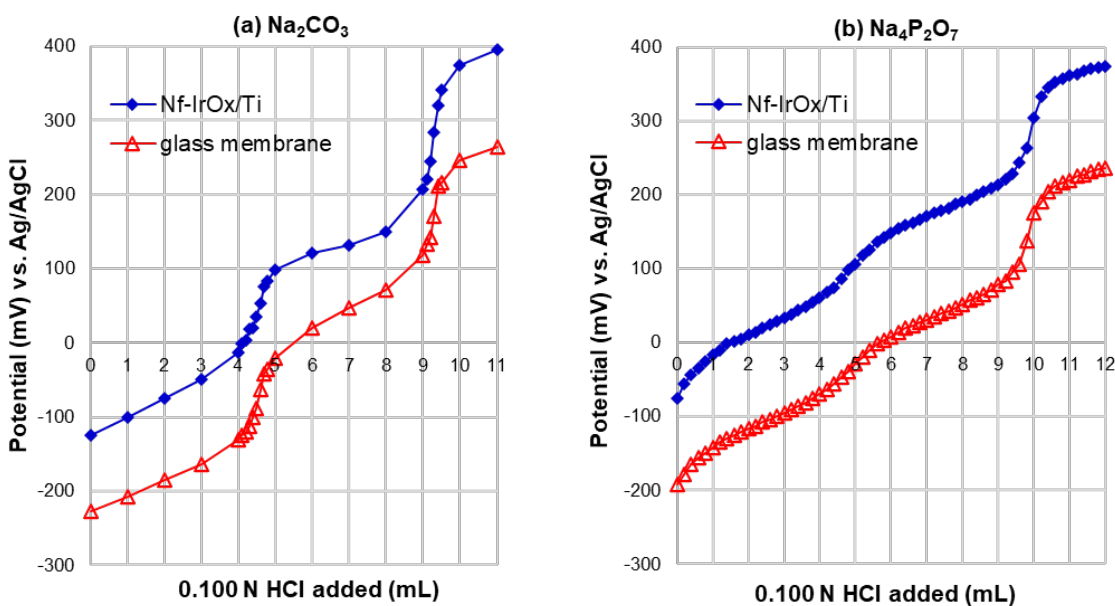

Figure 5: *Potentiometric titration curves between 0.100 N HCl and (a) Na_2CO_3 and (b) $Na_4P_2O_7$ using Nf-IrO$_x$/Ti and traditional glass membrane electrodes (Sentix-41 combination electrode)*

Table 1: *The equivalence points estimated from the titration curves by an interpolation method*

Type	Example	V_{eq} (mL) (glass membrane)	V_{eq} (mL) (Nf-IrO$_x$/Ti)	% Relative error
Strong acid by strong base	HCl – NaOH	4.65	4.66	+0.22 %
Polyprotic acid by strong base	H_3PO_4 – NaOH	4.39	4.35	−0.91 %
		8.83	8.93	+1.1 %
Polybasic base by strong acid	Na_2CO_3 – HCl	4.58	4.62	+0.87 %
		9.33	9.29	−0.43 %
	$Na_4P_2O_7$ – HCl	4.80	4.76	−0.83 %
		9.85	9.93	+0.81 %

The equivalence points could be estimated from the above titration curves by an interpolation method (using the Eq(1)) and summarized in Table 1. In most cases, the results showed the relative errors of less than 1 % compared to the glass membrane electrode. The tailor-made Nf-IrO$_x$/Ti electrode can be utilised as a pH sensor for the determination of the acidity or the alkalinity of an aqueous solution, as well as acid-base potentiometric titrations.

4. Conclusions

The present study proposed an easy-implementation and low-cost approach to fabricate iridium oxides coated on the titanium substrate for pH sensing purpose. The linear correlation between the potential response and the solution pH in the range of pH 2−12 was observed for both cases; the Nf-IrO$_x$/Ti electrode showed a longer equilibrium time (120 s) compared to the IrO$_x$/Ti electrode (60 s). The Nf-IrO$_x$/Ti as an indicator electrode was efficient in a potentiometric acid-base titration, showing the similarity in the curve shape, the steep rise in potential and the equivalence point compared to the glass membrane pH electrode, with less than 1 % relative errors. The promising results permit widening the application of the titanium-based iridium oxides electrode as a pH sensor for the determination of the acidity or the alkalinity of an aqueous solution, as well as acid-base potentiometric titrations.

Acknowledgments

References

Dang-Bao T., Le N.H., Lam H.H., 2022, Tuning Polyol-Mediated Process towards Augmentation of Zero-Valent Copper Nanoparticles, Chemical Engineering Transactions, 97, 331−336.

Fan K., Weisenhorn P., Gilbert J.A., Shi Y., Bai Y., Chu H., 2018, Soil pH correlates with the co-occurrence and assemblage process of diazotrophic communities in rhizosphere and bulk soils of wheat fields, Soil Biology and Biochemistry, 121, 185−192.

Harvey D. (Ed), 2000, Modern Analytical Chemistry, McGraw-Hill, New York, USA.

Huang W.D., Cao H., Deb S., Chiao M., Chiao J.C., 2011, A flexible pH sensor based on the iridium oxide sensing film, Sensors and Actuators A: Physical, 169, 1−11.

Jang H., Lee J., 2020, Iridium oxide fabrication and application: A review, Journal of Energy Chemistry, 46, 152−172.

Kim T.Y., Yang S., 2014, Fabrication method and characterization of electrodeposited and heat-treated iridium oxide films for pH sensing, Sensors and Actuators B: Chemical, 196, 31−38.

Mani G.K., Morohoshi M., Yasoda Y., Yokoyama S., Kimura H., Tsuchiya K., 2017, ZnO-Based Microfluidic pH Sensor: A Versatile Approach for Quick Recognition of Circulating Tumor Cells in Blood, ACS Applied Materials & Interfaces, 9, 5193–5203.

Manjakkal L., Szwagierczak D., Dahiya R., 2020, Metal oxides based electrochemical pH sensors: Current progress and future perspectives, Progress in Materials Science, 109, 100635.

Prats-Alfonso E., Abad L., Casañ-Pastor N., Gonzalo-Ruiz J., Baldrich E., 2013, Iridium oxide pH sensor for biomedical applications. Case urea–urease in real urine samples, Biosensors and Bioelectronics, 39, 163−169.

Ratanaporncharoen C., Tabata M., Watanagool N., Goda T., Matsumoto A., Sriyudthsak M., Miyahara Y., 2018, Characterization and Optimization of Thermally Grown Iridium Oxide and Its Application to pH Sensors, Sensors and Materials, 30, 1175−1185.

Salvoa P., Calisi N., Melai B., Cortigiani B., Mannini M., Caneschi A., Lorenzetti G., Paoletti C., Lomonaco T., Paolicchi A., Scataglini I., Dini V., Romanelli M., Fuoco R., Di Francesco F., 2017, Temperature and pH sensors based on graphenic materials, Biosensors and Bioelectronics, 91, 870–877.

Shylendra S.P., Wajrak M., Alameh K., 2023, Fabrication and Optimization of Nafion as a Protective Membrane for TiN-Based pH Sensors, Sensors, 23, 2331.

Xi Y., Guo Z., Wang L., Xu Q., Ruan T., Liu J., 2021, Fabrication and Characterization of Iridium Oxide pH Microelectrodes Based on Sputter Deposition Method, Sensors, 21, 4996.

Zhou Z., Li J., Pan D., Wei H., Wang C., Pan F., Xia J., Ma S., 2020, pH electrodes based on iridium oxide films for marine monitoring, Trends in Environmental Analytical Chemistry, 25, e00083.

Zhu L.Y., Li Y.C., Liu J., He J., Wang L.Y., Lei J.D., 2022, Recent developments in high-performance Nafion membranes for hydrogen fuel cells applications, Petroleum Science, 19, 1371−1381.